

A Contribution to the Ternary Phase Diagram Co – Sb – Te*

Peter Terzieff and Herbert Ipser

Institute of Inorganic Chemistry, University of Vienna, A-1090 Wien, Austria

Abstract. The melting behaviour, some phase boundaries and the lattice parameters in the region of the NiAs-type phase in the ternary system cobalt – antimony – tellurium have been determined by differential thermal analysis and X-ray diffraction. A projection of the liquidus surface and the phase relationships in different sections with constant antimony/tellurium ratios are presented. The peculiar variation of the lattice parameters with the composition of the nonstoichiometric NiAs-type phase is discussed in terms of the defect structure.

Keywords. Phase diagram: Co – Sb – Te; NiAs-type phase; Lattice parameter: Co – Sb – Te

Ein Beitrag zum ternären Phasendiagramm Co – Sb – Te

Zusammenfassung. Im Bereich der NiAs-Phase des ternären Systems Kobalt – Antimon – Tellur wurden mit Hilfe von thermischen Analysen und Röntgenbeugung das Schmelzverhalten, einige Phasengrenzen und Gitterparameter bestimmt. Neben einer Projektion der Liquidusoberfläche werden die Phasenbeziehungen in verschiedenen Schnitten mit konstanten Konzentrationsverhältnissen Antimon/Tellur vorgestellt. Die ungewöhnliche Variation der Gitterparameter mit der Zusammensetzung der nicht-stöchiometrischen NiAs-Phase wird anhand des Defektmechanismus erörtert.

Introduction

The appearance of phases with the hexagonal NiAs-(B8)-structure and that of a marcasite-(C18)-related structure is a common feature of the binary systems Co – Sb and Co – Te. Although the ternary phase diagram Co – Sb – Te seems to be well established [1] it was worth to supplement the existing results by additional measurements with emphasis on the range of the ternary NiAs-type phase.

It is a widely accepted view that the deviations from the ideal NiAs-type structure with the stoichiometry 1 : 1 are due to either vacant transition metal sites (subtractive type) or the insertion of additional transition metal atoms on interstitial sites (additive type). According to its cobalt deficiency Co_{1-x}Te represents the subtractive type of structure extending from about 55 to 64 at% Te [2–4] while the range of $\text{Co}_{1\pm x}\text{Sb}$, located around 50 at% Sb, includes both the subtractive and the additive version of the defect structure [5, 6].

* Dedicated to Prof. K. L. Komarek on the occasion of his 65th birthday

The careful analysis of the lattice parameters in $\text{Ni}_{1\pm x}\text{Sb}$, $\text{Co}_{1\pm x}\text{Sb}$ and $\text{Ni}_{1\pm x}(\text{Sb}, \text{Te})$ revealed a close relation between the individual type of defect mechanism and the sensitivity of the lattice parameters to changes in composition [6–8]. In this sense, the present paper is a continuation of our preceding studies on this very particular subject complemented by some additional aspects of the phase diagram.

Experimental

The alloys were prepared by direct reaction of the elements using Co wire (purity > 99.997%, Johnson-Matthey, U.K.) and antimony and tellurium lumps (purity > 99.99%, Asarco, New York). The appropriate mixtures (≈ 1 g) were evacuated, repeatedly flushed with purified argon, and finally sealed under vacuum (≈ 0.01 Pa) in quartz ampoules. After a first reaction period of about three days at 1350 K the ingots were rapidly cooled to room temperature, crushed in ground, subjected again to repeated evacuating-flushing cycles, and once more sealed in quartz ampoules. In order to achieve homogeneity the alloys were thermally treated at 1150 K for about two weeks. The well homogenized powders were quenched in ice water and their phase purity and structure were determined by X-ray diffraction. The diffraction patterns were taken in 57.30 mm Debye-Scherrer cameras using $\text{Co-K}\alpha$ -radiation and Fe-filters.

Thermal effects were traced on a commercial thermal analyzer (DTA 404S/3), Netzsch, Selb, F.R.G.) using samples of about 0.5 g sealed under vacuum in special quartz containers. An empty alumina crucible was used as reference. Except for some special cases, the heating and cooling rate was 2 K min^{-1} . The temperature was determined with a Pt/Pt–Rh (10% Rh) thermocouple calibrated at the melting points of high purity zinc, antimony and gold.

Results and Discussion

Four different series of alloys were prepared with constant $x_{\text{Sb}}/x_{\text{Te}}$ ratios of 0.33, 1, 3, and 7. The compositions of the alloys and the results of the thermal analyses

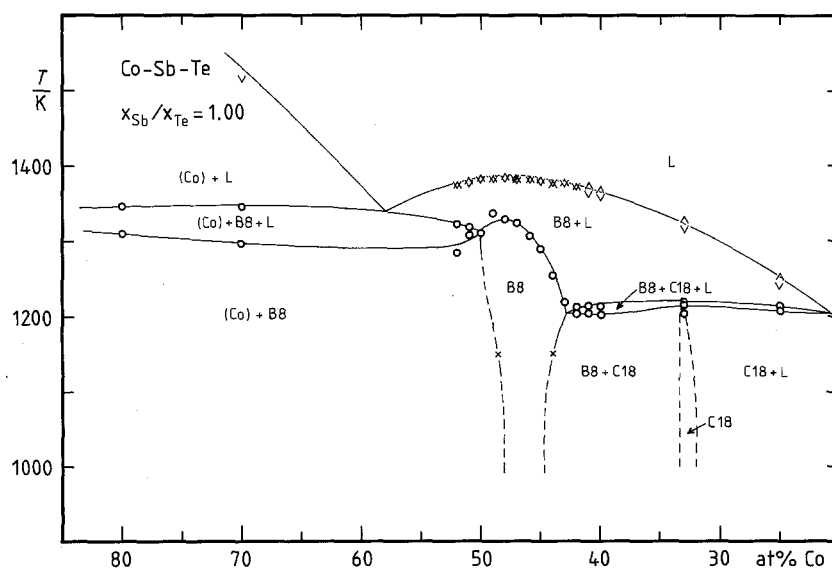


Fig. 1. Phase boundaries in the isopleth with $x_{\text{Sb}}/x_{\text{Te}} = 1$. \blacktriangle , \blacktriangledown liquidus on heating and cooling; \circ solidus and other thermal effects; \times phase width deduced from lattice parameters

are listed in Table 1 together with the lattice parameters of the hexagonal-(NiAs)-phase (a , c) and those of some samples with the orthorhombic marcasite-phase (a , b , c).

The interpretation of the thermal effects and the resulting phase relationships in the isopleth with $x_{\text{Sb}}/x_{\text{Te}} = 1$ are presented in Fig. 1 covering the full composition range of Co investigated in this paper (25–80 at% Co). Those in the isopleths with $x_{\text{Sb}}/x_{\text{Te}} = 0.33$ and 3 are shown only for the vicinity of the B8-phase (Fig. 2) in combination with the equivalent binary phase fields taken from the literature [3, 6].

Due to the likeness of the binary phase diagrams – a congruently melting B8-type phase and a peritectically formed C18-type phase [3, 6] – the appearance of the different phase fields remains the same throughout the ternary system, and the changes from one isopleth to the other are only gradual. According to the different stability ranges of the binary B8-phases we observed a systematic change in the phase boundaries and in the position of the liquidus maximum. In the sequence of $x_{\text{Sb}}/x_{\text{Te}} = 0, 0.33, 1, 3$ and ∞ the liquidus maximum occurs successively at 1288, 1328, 1388, 1440, and 1493 K being located at 43.8, 46.0, 48.5, 50.0, and

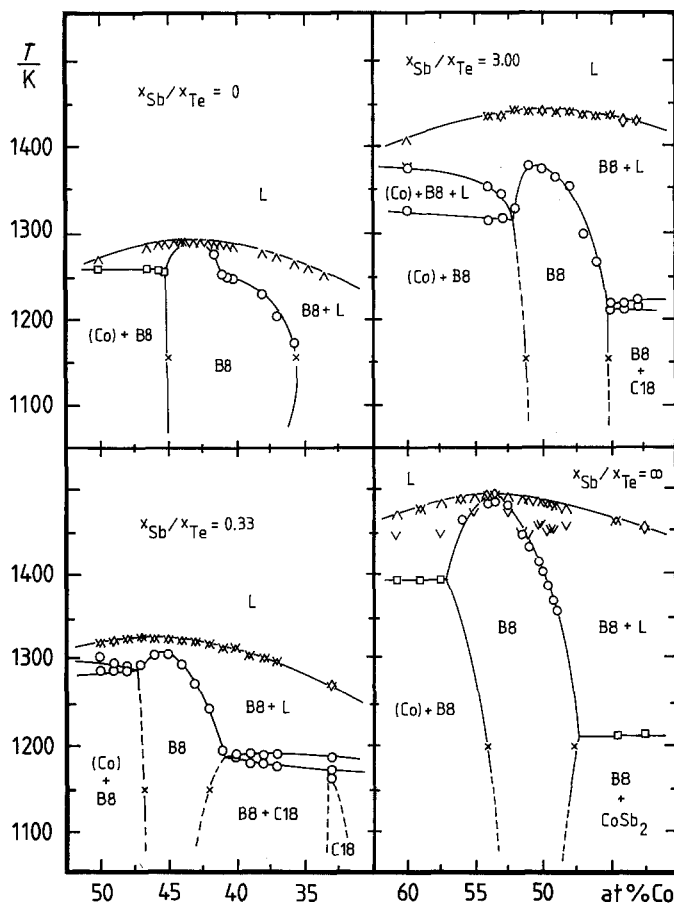


Fig. 2. The phase width of the B8-type phase in the binary systems [3, 6] and in the isopleths with $x_{\text{Sb}}/x_{\text{Te}} = 0.33$ and 3. Δ , ∇ liquidus on heating and cooling; \circ solidus and other thermal effects; \times phase with deduced from lattice parameters

53.5 at% Co, respectively. At 1150 K – our reference temperature for the lattice parameters – the range of homogeneity shifts progressively from 36.5–44.7 to 42–47, 44–48.5, 45–51, and 47.4–54.8 at% Co.

A projection of the liquidus surface and the variation of the peritectic and the eutectic troughs across the ternary phase field are shown in Fig. 3. As already apparent from Fig. 2, the system shows a very simple melting behaviour. Both the eutectic and the peritectic trough as well as the liquidus surface itself rise in a continuous manner from the Te-rich towards Sb-rich side. As far as comparable to previous investigations in this system [1] it has to be noted that the form of the liquidus surface and the phase relationships are in principal agreement with our findings. In fact, the phase boundaries reported for the section from Co to Sb_2Te_3 have a strong resemblance to the isopleths presented in this paper (cf. Fig. 2), and even the somewhat distorted form of the B 8-phase field is almost the same as that of our isopleth with $x_{\text{Sb}}/x_{\text{Te}} = 1$ (cf. Fig. 1).

The variation of the lattice parameters (a , c), the axial ratio (c/a), and the volume of unit cell (V) with the composition of the B 8-type phase is shown in Fig. 4 a–d. The additional isopleth with $x_{\text{Sb}}/x_{\text{Te}} = 7$ has been prepared in order to elaborate some of the details on the antimony-rich side of the system.

The separately marked discontinuities in the lattice parameters manifest the phase boundaries which have also been included in Fig. 1 and Fig. 2. As to the width itself, we observed a narrowing of the ternary phase field around $x_{\text{Sb}}/x_{\text{Te}} = 1$. The numerical values are already discussed in a previous section of this paper.

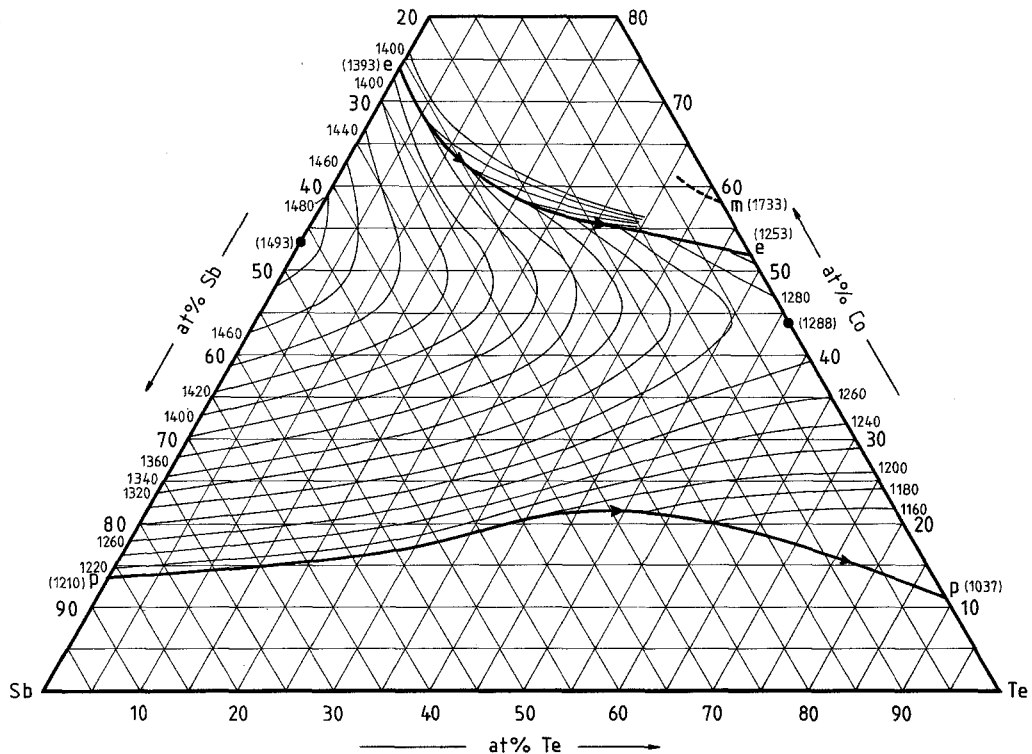


Fig. 3. Projection of the liquidus surface in the Co–Sb–Te system. e binary eutectic point, p binary peritectic point, m binary monotectic, ● congruent melting point

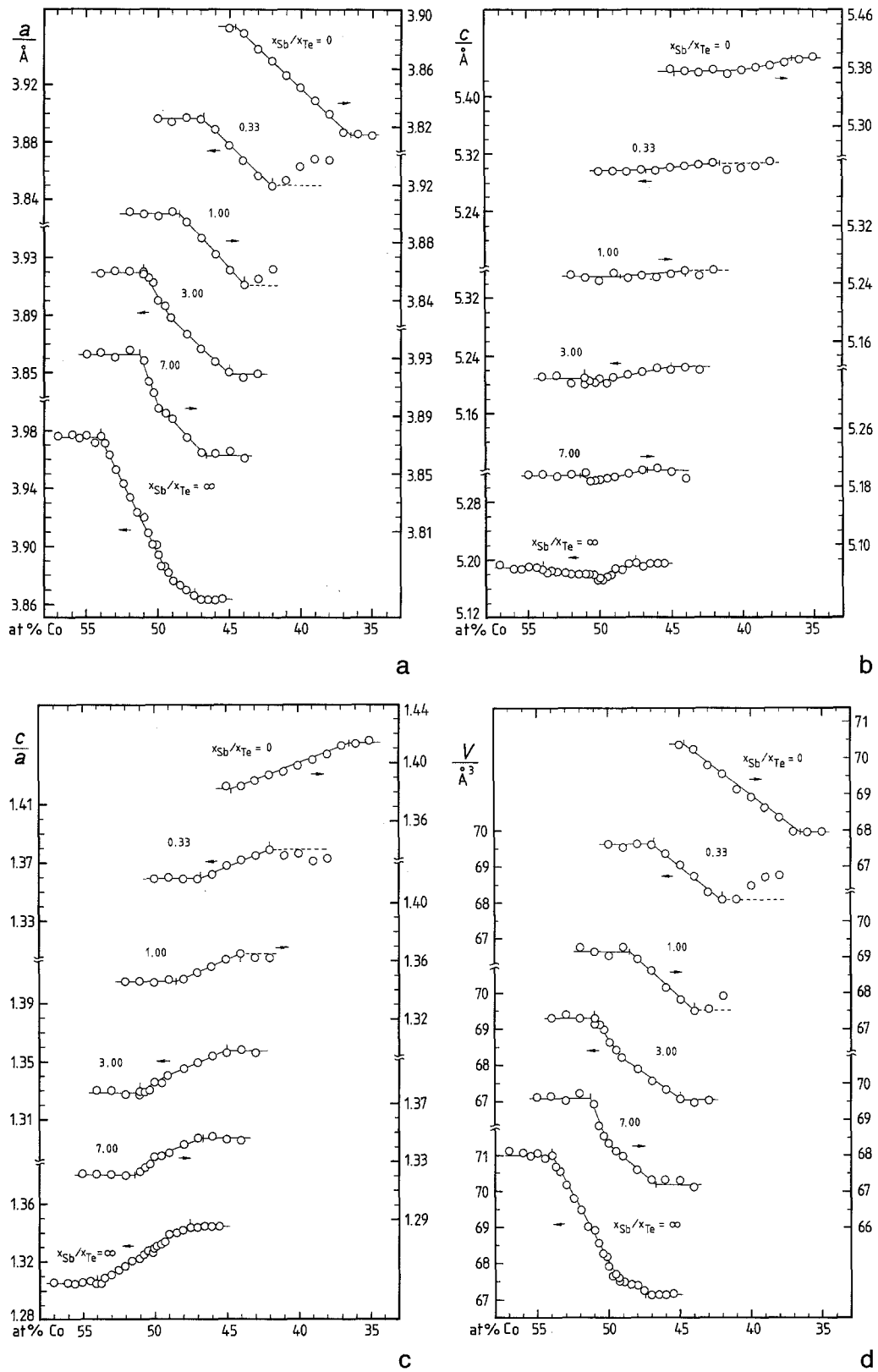


Fig. 4 a-d. Variation of the lattice parameters a and c , the axial ratio c/a , and the unit cell volume V in the binary systems [4, 6] and in four isopleths with $x_{Sb}/x_{Te} = 0.33, 1, 3, \text{ and } 7$ (1150 K)

Table 1. Composition, lattice parameters, liquidus and solidus temperatures, and other thermal effects in ternary Co–Sb–Te alloys

Composition			Liquidus		Solidus	Others	Lattice Parameter		
No.	x_{Sb} x_{Sb}	at%Co	(↑)	(↓)	(↑) (K)	(↑)	<i>a</i>	<i>b</i> (Å)	<i>c</i>
51	7.00	44.0	1453	1438		1196–1205	3.861		5.192
52		45.0					3.866		5.201
53		46.0	1461	1451		1197–1208	3.864		5.207
54		47.0					3.865		5.204
55		48.0	1461	1445	1328		3.875		5.199
56		49.0					3.888		5.195
94		49.5					3.892		5.193
57		50.0	1468	1454	1403		3.899		5.191
95		50.3					3.906		5.189
96		50.7					3.914		5.188
58		51.0					3.928		5.196
59		52.0	1467	1455	1420		3.936		5.198
60		53.0					3.931		5.195
61		54.0	1464	1447	1397		3.934		5.198
62		55.0					3.933		5.198
82	3.00	25.0	1303	1285		1197–1204; a			
75		33.0	1371	1359		1198–1211; a	5.376	6.301	3.633
40		43.0	1431	1418		1209–1218	3.850		5.221
2		44.0	1431	1415		1207–1213	3.847		5.226
3		45.0	1437	1428		1206–1215	3.851		5.222
4		46.0	1435	1428	1261		3.858		5.224
5		47.0	1437	1430	1294		3.867		5.218
6		48.0	1439	1432	1350		3.887		5.215
7		49.1	1438	1433	1360		3.888		5.211
97		49.5					3.897		5.203
8		50.0	1442	1431	1370		3.900		5.210
98		50.3					3.913		5.204
99		50.7					3.916		5.206
9		51.0	1440	1432	1374		3.919		5.210
10		52.0	1441	1434	1323		3.921		5.203
11		53.0	1435	1424		1313–1340	3.921		5.213
12		54.0	1434	1428		1310–1349	3.919		5.212
83		60.0	1406	1368		1322–1371			
84		70.0	1472	1446		1340–1379; a			
85		80.0		>1530		1349–1378			
87	1.33	63.0	n.o.	1400		1317–1360			
86	1.00	25.0	1257	1235		1208–1214; a			
76		33.0	1333	1311		1216–1220; a	5.250	6.244	3.826
13		40.0	1372	1354		1203–1214			
14		41.0	1378	1359		1205–1215			
15		42.0	1376	1368		1204–1213	3.862		5.259
16		43.0	1382	1372	1219		3.855		5.251
17		44.0	1379	1373	1255		3.851		5.258
18		45.0	1385	1375	1290		3.861		5.254

Composition			Liquidus		Solidus	Others	Lattice Parameter		
No.	$\frac{x_{Sb}}{x_{Sb}}$	at%Co	(↑)	(↓)	(↑) (K)	(↑)	<i>a</i>	<i>b</i> (Å)	<i>c</i>
19		45.9	1 385	1 376	1 307		3.872		5.249
42		47.0	1 385	1 377	1 324		3.884		5.253
20		47.1	1 358	1 382	1 321		3.884		5.253
21		48.0	1 390	1 378	1 329		3.895		5.248
22		49.0	1 388	1 379	1 337		3.902		5.225
23		50.0	1 388	1 377	1 311		3.899		5.244
24		51.0	1 385	1 372		1 308–1 319	3.900		5.249
25		52.0	1 380	1 371		1 285–1 323	3.902		5.253
88		70.0	n.o.	1 511		1 298–1 346			
89		80.0		> 1 530		1 310–1 347			
90	0.33	25.0	1 204	1 184		1 159–1 170; a			
77		33.0	1 276	1 261		1 171–1 185; a	5.273	6.266	3.884
26		37.0	1 300	1 293		1 174–1 189	3.878		5.294
27		38.0	1 305	1 294		1 177–1 188	3.867		5.310
28		39.0	1 307	1 300		1 177–1 190	3.868		5.303
29		49.1	1 315	1 311		1 185–1 189	3.863		5.300
30		41.0	1 315	1 310	1 194		3.853		5.297
31		42.0	1 319	1 314	1 241		3.849		5.308
32		43.0	1 324	1 317	1 271		3.856		5.304
33		44.0	1 325	1 317	1 294		3.867		5.303
34		45.0	1 328	1 318	1 306		3.878		5.301
35		46.0	1 328	1 318	1 306		3.889		5.296
36		47.0	1 330	1 320	1 293		3.896		5.298
37		48.0	1 328	1 322		1 286–1 293	3.897		5.295
38		49.0	1 326	1 317		1 286–1 296	3.894		5.296
39		50.0	1 322	1 316		1 286–1 303	3.896		5.296
91		60.0	n.o.	1 501		1 274–1 310			
92		70.0		> 1 530		1 281–1 303			
93		80.0		> 1 530		1 284–1 304			

↑ heating; ↓ cooling; *a* additional thermal effect(s); *n.o.* not observed

In general, the *hcp* metalloid sublattice of the B8-structure is assumed to be invariable, i.e. completely filled throughout the range of homogeneity, thus any increase in transition metal content implies a filling up of the structure, irrespective of the prevailing type of defect. As a consequence, it is not surprising to find both *a* and *V* expanding with increasing Co-content. Along the *c*-axis, this effect is possibly compensated by increased direct bonding interactions between neighbouring Co atoms, however, the trends in *c* are very weak and the interpretation is tentative.

The most striking feature of the lattice parameter vs. composition curves is the change of the slope around 50 at%Co clearly apparent for *a* and *V*, and less pronounced for *c*. It is obvious to attribute this to the transition from the subtractive (cobalt deficient) to the additive type of defect structure (cobalt atoms in interstices) which is expected to occur at about the stoichiometric composition (1 : 1). On the

cobalt-deficient side ($x_{\text{Co}} < 0.5$) the filling up occurs via the octahedral holes of the *hcp* (Sb, Te)-network, up to the stoichiometry of 1 : 1. The additional cobalt atoms on the cobalt-rich side ($x_{\text{Co}} > 0.5$) are positioned on the smaller bipyramidal sites of the structure. Accordingly, it is a consequence of the space requirements that the lattice expansion is more pronounced for the additive type of the structure.

All this is in good agreement with conclusions drawn in the preceding articles on the systems Ni – Sb, Co – Sb, and Ni – Sb – Te [6–8] where we also found two definitely different slopes reflecting the difference in defect mechanism.

Taking the cell volume – in general the most pronounced parameter – as measure of the lattice expansion we may assign the average slope of about 0.3 \AA^3 per atomic percent to the subtractive type and 0.8 \AA^3 per atomic percent to the additive type of structure. Furthermore, it is once more interesting to note that the range covered by the volume of the unit cell – extending from about 67 to 71 \AA^3 – remains the same throughout the ternary phase field of both Co – Sb – Te and Ni – Sb – Te.

All in all, the coincidences are certainly remarkable, however, the differences in size between cobalt and nickel are only small and the significance of the argumentation for the whole class of NiAs-phases is doubtful. We may also state that some of the trends observed in the lattice parameters are explicable in terms of very elementary concepts, but we also admit that some of the details are still not completely understood.

Acknowledgement

The authors thank Ms. A. Havlicek as well as Mr. P. Krajnik and Mr. A. Karka for their help during one of their laboratory courses, and Prof. K. L. Komarek for critically reviewing this article.

References

- [1] Abrikosov N. Kh., Petrova L. I. (1978) *Izv. Akad. Nauk SSSR, Inorg. Mater.* **14**: 346
- [2] Haraldsen H., Gronvold F., Hurlen T. (1956) *Z. Anorg. Allg. Chemie* **283**: 143
- [3] Klepp K. O., Komarek K. L. (1973) *Monatsh. Chem.* **104**: 105
- [4] Schicketanz H., Terzieff P., Komarek K. L. (1986) *J. Less-Common Met.* **119**: 13
- [5] Kjekshus A., Walseth K. P. (1969) *Acta Chem. Scand.* **23**: 2621
- [6] Hanninger G., Ipser H., Terzieff P., Komarek K. L. (1990) *J. Less-Common Met.* **166**: 103
- [7] Leubolt R., Ipser H., Terzieff P., Komarek K. L. (1986) *Z. Anorg. Allg. Chem.* **533**: 205
- [8] Ipser H., Terzieff P. (1986) *Monatsh. Chem.* **117**: 729

Received April 10, 1991. Accepted July 24, 1991